EMMA—A Geophysical Training and Education Tool for Electromagnetic Modeling and Analysis

Esben Auken, Lars Nebel, Kurt Sørensen, Morten Breiner, Louise Pellerin*, and Niels B. Christensen
The HydroGeophysics Group, Department of Earth Sciences, University of Aarhus, Finlandsgade 8, DK-8200 Aarhus N, Denmark

ABSTRACT

An interactive modeling and analysis program with a user-friendly graphical interface, for students and professionals in the field of exploration geophysics, has been developed. The ElectroMagnetic Modeling and Analysis program—EMMA—is capable of modeling one-dimensional responses for most electrical and electromagnetic methods and array configurations, including the time-domain, frequency-domain, resistivity, magnetotelluric and borehole methods. EMMA is available on-line, at no charge, from http://www.hgg.au.dk.

An innovation of EMMA is the calculation of the model sensitivity analysis, a feature that is usually only present in inversion codes. The variance of the model parameters depends on the variance of the measured data and the way in which an error is mapped from the data to the model parameters. The measurement situation is realized by ascribing data noise to the model response. This facilitates the calculation of a realistic model parameter analysis. For time-domain data, piecewise linear waveforms, ramps and low-pass filters are included in the forward modeling scheme.

When implemented on a multi-user relational database structure, EMMA is suitable for classroom exercises where the computers are connected through a local network. As an illustration and for motivation, three exercises focusing on the time-domain electromagnetic method are presented: the mapping of noise to model resolution; the effect of filters on the early time response and layer resolution; and an examination of the electric and magnetic field intensity to understand the physical mechanisms of the method.

Short courses on the subject of the transient electromagnetic and resistivity methods for hydrogeophysical investigations, offered to technical advisers and to technical policy-makers, have demonstrated EMMA's succes in providing a productive learning environment.

Introduction

In recent years, electrical and electromagnetic (EM) geophysical methods have been widely used by geologists, engineers and hydrologists in environmental, geotechnical and hydrological investigations. The understanding and quantitative description of the possibilities and limitations of one-dimensional (1D) interpretation of electromagnetic and resistivity data remains a non-trivial intellectual task for present and future professionals working within the geophysical community. For accurate design, acquisition and interpretation of field experiments, an advanced knowledge level is required. Modeling is a recognized method to acquire such specialized knowledge.

An interactive ElectroMagnetic Modeling and Analysis (EMMA) program has been developed as part of a training initiative to enhance skills in project design and project solutions. EMMA is a MS-Windows based user-friendly graphical interface (GUI) to a 1-D modeling and analysis code. EMMA is available on-line[1], at no fee, for use by students and professionals in the geophysical community.

Some educational and web access codes are already available. Bankey and Anderson (1995) have released a variety of EM and potential field modeling and inversion algorithms as US Geological Open-File Reports. These codes are free to the user, but do not have user-friendly interfaces; the user must be able to compile, link and possibly debug FORTRAN codes. Academic modeling consortiums, such as the IMAGE Consortium at the University of British Columbia (Oldenburg, 2001), the University of Utah CEMI (Zhdanov, 2001), and the CSIRO EM Modelling Program (Raiche, 2001), support research and development, but ac-

* Currently at the University of Utah, Energy and Geoscience Institute, Salt Lake City, Utah, USA.

[1] Emma is available from www.hgg.au.dk at no charge for the international geophysical community. People are encouraged to make an online registration of EMMA. HGG offers to email a notification when a new enhanced version of the program becomes available.

cess to these modeling codes requires a significant monetary commitment often extending over several years.

Boyd and Romig (1997) designed a computer-based learning environment for use in cross-disciplinary earth-science education. Computer simulations allow students to interact with all aspects of a geophysical problem. This helps them to become comfortable with the thought processes employed by a specialist and to develop an intuitive understanding of the underlying physics. Pinto *et al.* (2000) developed interactive teaching software for potential fields in applied geophysics. The program is written in Visual Basic with some subroutines in FORTRAN for the MS-Windows environment. The program offers the majority of the processes involved in geophysical data handling and modeling for the magnetic and electrical resistivity methods.

EMMA is dedicated to problems related to the use of electric and electromagnetic methods. In the following sections, we briefly discuss the EM and inversion theory on which EMMA and the FORTRAN95 program, used to compute the model response and analysis, are based. Subsequently, we give an overview of the GUI structure.

To demonstrate the use of EMMA, we have constructed three examples for the time-domain electromagnetic method (TEM): 1) the effect of data noise on model resolution; 2) the effect of low-pass filters in TEM measurements; and 3) a presentation of the TEM fields in the ground. Finally we discuss our experiences from using EMMA in a TEM short course arranged for consultants working with problems related to hydrogeophysics.

Theory

The mathematical formulation of the one-dimensional electromagnetic problem is described in detail in Ward and Hohmann (1988). The solution is computed in the frequency domain using the digital Hankel transform theory of Johansen and Sørensen (1979) and filters computed by Christensen (1990). The transient responses are calculated from the frequency domain responses using a Fourier transform computed as a cosine or sine transform using digital filters (Anderson, 1975; Newman *et al.,* 1986). This approach is slightly more computer intensive than the commonly used Gaver-Stehfest inverse Laplace transform (Knight and Raiche, 1982), but we found the Fourier transform to be more stable and accurate at late times.

The derivation of the finite-loop and dipole sources follows that developed by Newman *et al.* (1986), where a loop is divided into small, ungrounded electric dipole elements and numerically integrated. The ground terms are computed separately and added as source terms for the finite line source.

The electrical resistivity formulation follows that of Telford *et al.* (1995).

The forward modeling codes were successfully tested and verified against existing codes. The loop source responses were compared to those of Newman *et al.* (1986). The time-domain transform and the resistivity calculations were verified with the code of Christensen and Auken (1992). The magnetotelluric as well as the finite and infinite line source responses were tested against an in-house modeling code at Lawrence Berkeley National Laboratory (G. Michael Hoversten and K. H. Lee, personal communication). Appendix A summarizes supported transmitter-receiver configurations and estimates of the numerical accuracy of the response functions

Providing a model parameter uncertainty analysis, as defined by geophysical inverse theory (Menke, 1989), EMMA is well suited for performing experimental design. Conventional 68% probability error bars, *i.e.,* intervals typically containing each model parameter, are computed based on the uncertainty of the method and the uncertainty in the observational data. In EMMA, data are produced by ascribing user-defined noise intervals on the model response. Parameter uncertainty (standard deviation, STD) is calculated as the square root of the diagonal elements, σ^2, from the covariance matrix of the inverse estimation. This estimation error covariance matrix is computed from sensitivities of the model parameters and data error covariance matrix (Jackson, 1979; Tarantola and Valette, 1982).

Model resistivities and thicknesses are represented by their logarithms for stability and as a positivity constraint (Johansen, 1977). This means that the standard deviation on each model parameter (resistivity, thickness and depth) is calculated as a standard deviation factor (STDF). Hence, it is 68% probable that a given model parameter m_j falls within an interval between $m_j/STDF_j$ and m_j*STDF_j. Thus, the impossible case of perfect resolution has an STDF = 1, moderate to well resolved parameters have an STDF < 2, and unresolved parameters an STDF > 2.

An analysis can be performed on one or more data types. This means that *e.g.,* two data sets may be used to constrain a model simultaneously, allowing for experimental design of joint inductive and galvanic exploration (Jupp and Vozoff, 1977).

EMMA Structure

EMMA handles most electrical and electromagnetic transmitter-receiver configurations. All transmitter configurations can be located in the air or on the earth's surface. The vertical magnetic dipole (VMD) and the vertical electric dipole (VED) are also allowed to be in the earth. Receivers are permitted anywhere for all field components. For any source, time domain data can be computed as the electric field, E, the magnetic field, H, the magnetic field intensity, B, their time derivatives and apparent resistivity for a user-defined waveform and system response. Frequen-

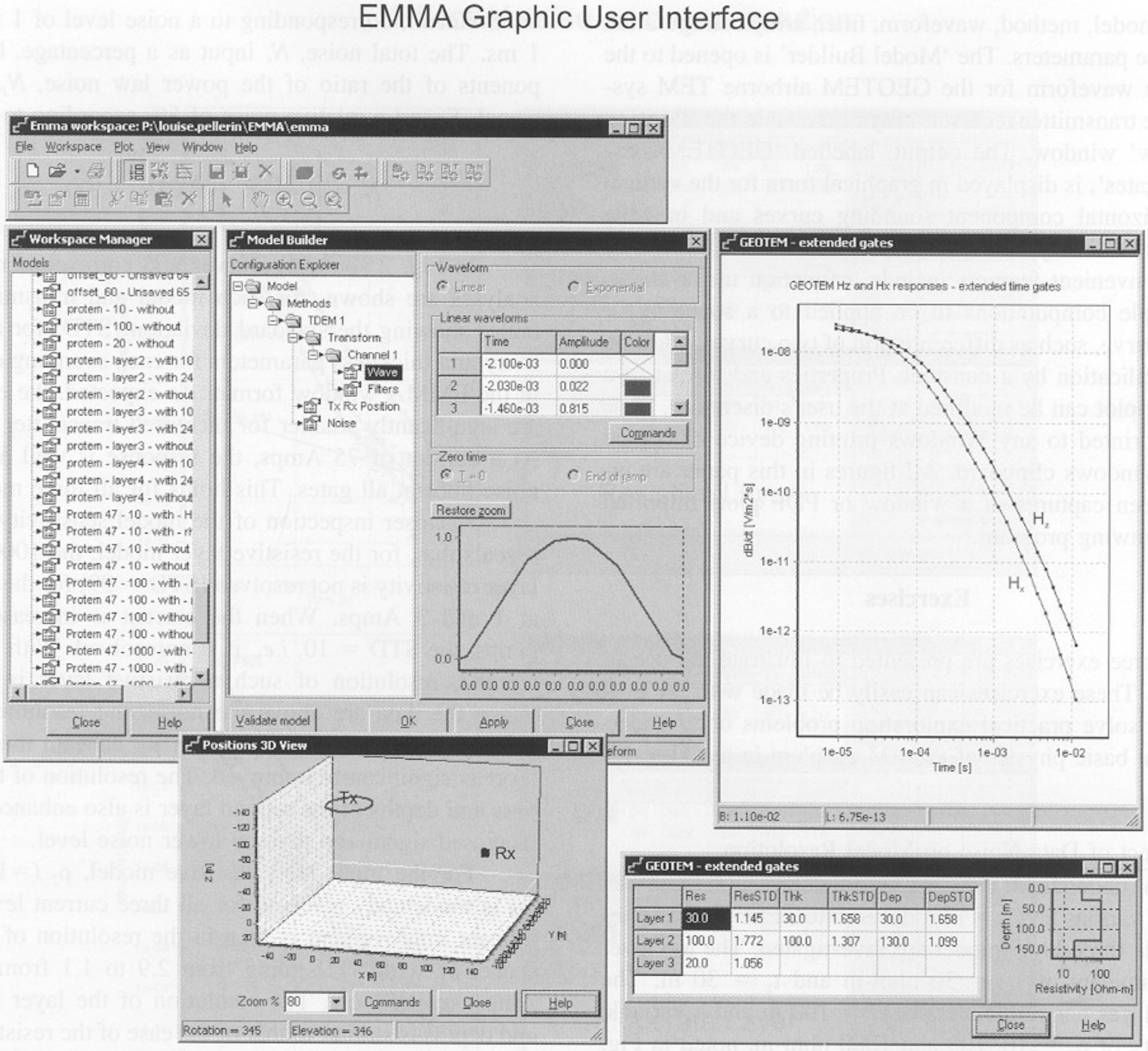

Figure 1. A collage of windows from an EMMA workspace showing the GEOTEM wave form, 3-D array configuration, magnetic response for the vertical and horizontal components of the 3-layer model, and analysis of the layer resistivity, thickness, and depths for the vertical component.

cy domain responses are reported as the in-phase and quadrature in parts per million (PPM) or percent of the primary field, or as amplitude and phase. Magnetotelluric (MT) responses, including controlled-source audio MT, are calculated as apparent resistivity and phase, or normalized field values of E and H. For any array on the earth, electrical resistivity responses are given as apparent resistivity. Please refer to Appendix A for a complete list of supported source-receiver configurations.

For time domain data, realistic waveforms, ramps and filters are essential to accurately model and analyze field systems (Raiche, 1984; Fitterman and Anderson, 1987; Asten, 1987; Effersø *et al.*, 1999). Therefore, this set of parameters, defining the TEM system transfer function, is part of the input construction and can be configured to model any transmitter-receiver system.

EMMA builds upon a multi-user relational database structure—referred to as the EMMA workspace. The multi-user database makes the program particularly suitable for classroom exercises where the computers are connected through a local network. Because all parameters used to set up the models are saved in the workspace, the user is not concerned with inputting correctly formatted ASCII files or running DOS programs. The workspace remains open until explicitly closed; there are no files to open or save. Standard Windows functionality within EMMA, such as 'cut and paste' commands or selecting curves with a mouse click, makes for an immediate familiarity and minimizes the learning curve.

Figure 1 shows an open 'Workspace' with the windows of the 'Workspace Manager' and the 'Model Builder'. The "Model Builder" is used to set up the input options for the model, method, waveform, filter, array configuration and noise parameters. The 'Model Builder' is opened to the half-sine waveform for the GEOTEM airborne TEM system. The transmitter-receiver array is shown in the 'Position 3D View' window. The output, labelled 'GEOTEM—extended gates', is displayed in graphical form for the vertical and horizontal component sounding curves and in table form for the analysis.

Convenient features include a function menu allowing simple computations to be applied to a sounding or profile curve, such as differentiation of two curves, addition or multiplication by a constant. Properties and format of a curve or plot can be modified at the user's discretion. Plots can be printed to any Windows printing device or copied to the Windows clipboard. All figures in this paper are either screen captures of a window or PDF plots imported into a drawing program.

Exercises

Three exercises are presented to illustrate the use of EMMA. These exercises can easily be made with the program to solve practical exploration problems or to understand the basic physics of the EM problem in teaching situations.

The Effect of Data Noise on Model Resolution

To understand changes in model resolution when noise of various levels is introduced into TEM data, a series of simple three-layer model are investigated. The top layer has parameters of $\rho_1 = 30$ ohm-m and $t_1 = 30$ m. The second layer has a thickness of $t_2 = 100$ m and a variable resistivity of $\rho_2 = 10$, 100 and 1000 ohm-m, noted in Fig. 2, as conductive, moderate and resistive, respectively. The resistivity of the bottom half space is $\rho_3 = 20$ ohm-m. The array is that of a 40 by 40 m central-loop configuration on the surface of the earth. For each model, three transmitter currents are used: (a) 1 Amp, (b) 3 Amps and (c) 75 Amps. The transmitted waveform is a modified square wave with a finite ramp of 2.5 μsec.

For the noise model, a power law distribution is used so that

$$N_{PL} = bt^{a} \qquad (1)$$

where a and b are constants to be defined for a given system. Munkholm and Auken (1996) found typical values for a Geonics Ltd. PROTEM 47 system (Geonics, 2001) to be $a = -0.5$ and $b = 3 \times 10^{-11}$ in a densely cultivated rural environment, corresponding to a noise level of 1 nV/m² at 1 ms. The total noise, N, input as a percentage, has components of the ratio of the power law noise, N_{PL}, to the signal, S, and a relative noise of 5% according to

$$N = \left[\left(\frac{N_{PL}}{S}\right)^2 + 0.05^2\right]^{1/2} \cdot 100 \qquad (2)$$

In Fig. 2 sounding curves and corresponding model analyses are shown, for each model and transmitter. The tables showing the standard deviation (STD) for the resistivity and thickness parameters for each sounding curve are in the EMMA window format. As expected, the error bars are significantly smaller for increased transmitter currents. At a current of 75 Amps, the response is well above the noise floor at all gates. This holds for all three models.

A closer inspection of the model sensitivity analysis reveals that, for the resistive layer model, the 1000 ohm-m layer resistivity is not resolved (STD = 99) for the response at 1 and 3 Amps. When the current is increased to 75 Amps, the STD = 10, *i.e.,* it is unresolved. With the TEM method, resolution of such a resistive layer is difficult. When the data are above the noise, the resolution of the resistivity of the basal half-space, ρ_3, beneath the resistive layer is significantly improved. The resolution of the thickness and depths of the second layer is also enhanced by the increased signal and thereby lower noise level.

For the moderately resistive model, ρ_2 (=100 ohm-m) is moderately resolved for all three current levels. Significant improvement is seen in the resolution of the half-space, ρ_3, with STD going from 2.9 to 1.1 from 1 to 75 Amps, respectively. The resolution of the layer thickness and depths is similar to that of the case of the resistive layer, *i.e.,* moderate to good.

The situation is different when the middle layer becomes conductive. For all three responses, the top two layer resistivities are well resolved, as would be expected because the TEM method is optimal for determining conductive structures. Resolution of layers beneath a conductor is difficult, but is achieved for the 75 Amps response with a STD = 1.4 for ρ_3. For 1 and 3 Amps, ρ_3 are unresolved with a STD of 10 and 3.4, respectively. The TEM method is known to resolve the top, not the bottom, of a conductor. Resolution of thickness and depths of layer 2 is not as good resolved as in the previous cases of a resistive middle layer. However, increasing the signal above the noise level increases resolution of these parameters.

It is common knowledge that increasing signal

→

Figure 2. The effect of noise on data resolution. Voltage soundings, with error bars, and analysis tables for 3 three-layer earths and 3 transmitter currents—(a) 1 Amp, (b) 3 Amps, and (c) 75 Amps. The noise model is also shown on the sounding curves.

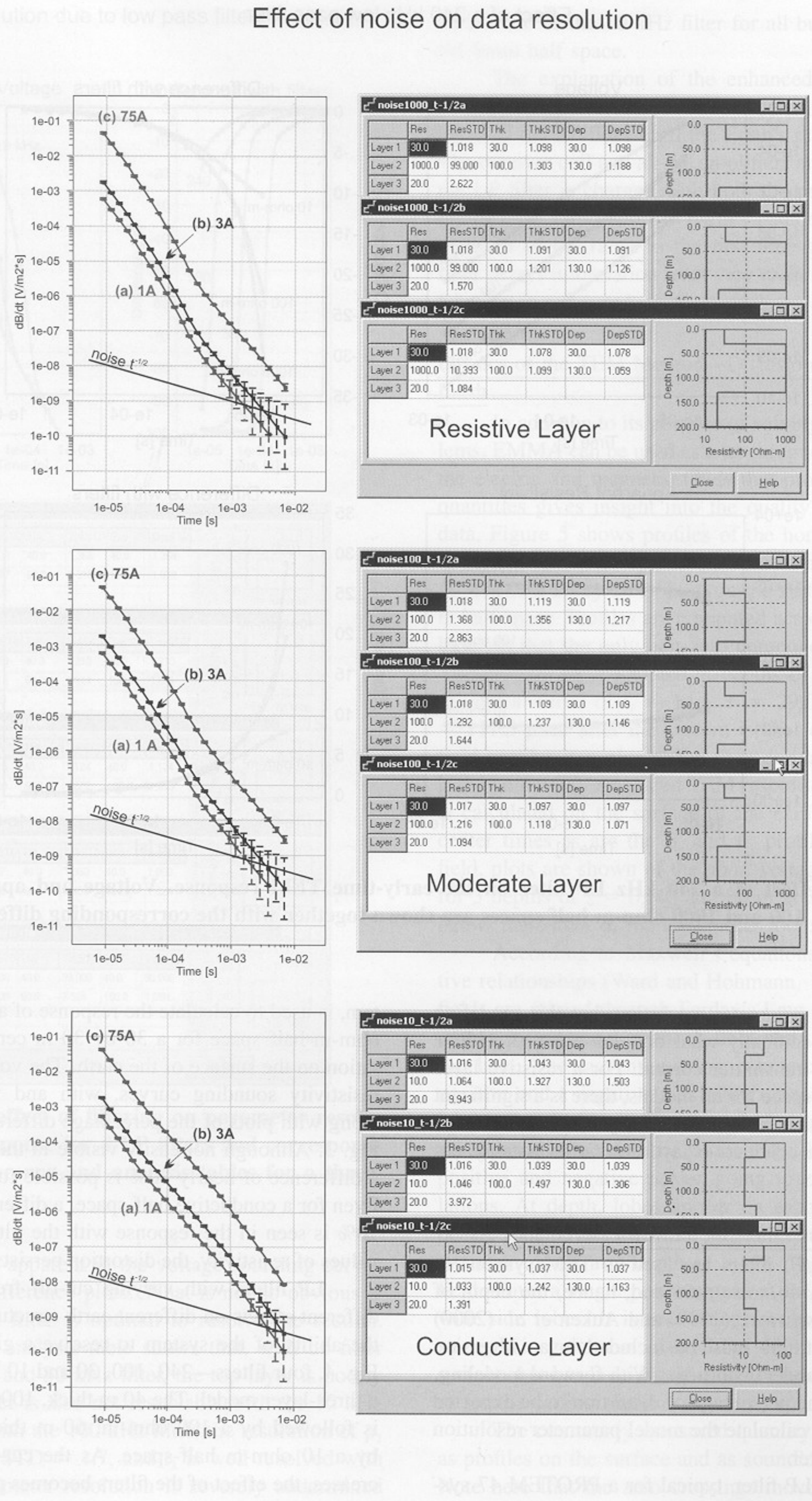
Effect of noise on data resolution
(c) 75A
(b) 3A
(a) 1A
noise $t^{-1/2}$
dB/dt [V/m2*s]
Time [s]
noise1000_t-1/2a
Res ResSTD Thk ThkSTD Dep DepSTD
Layer 1 30.0 1.018 30.0 1.098 30.0 1.098
Layer 2 1000.0 99.000 100.0 1.303 130.0 1.188
Layer 3 20.0 2.622
noise1000_t-1/2b
Layer 1 30.0 1.018 30.0 1.091 30.0 1.091
Layer 2 1000.0 99.000 100.0 1.201 130.0 1.126
Layer 3 20.0 1.570
noise1000_t-1/2c
Layer 1 30.0 1.018 30.0 1.078 30.0 1.078
Layer 2 1000.0 10.393 100.0 1.099 130.0 1.059
Layer 3 20.0 1.084
Resistive Layer
noise100_t-1/2a
Layer 1 30.0 1.018 30.0 1.119 30.0 1.119
Layer 2 100.0 1.368 100.0 1.356 130.0 1.217
Layer 3 20.0 2.863
noise100_t-1/2b
Layer 1 30.0 1.018 30.0 1.109 30.0 1.109
Layer 2 100.0 1.292 100.0 1.237 130.0 1.146
Layer 3 20.0 1.644
noise100_t-1/2c
Layer 1 30.0 1.017 30.0 1.097 30.0 1.097
Layer 2 100.0 1.216 100.0 1.118 130.0 1.071
Layer 3 20.0 1.094
Moderate Layer
noise10_t-1/2a
Layer 1 30.0 1.016 30.0 1.043 30.0 1.043
Layer 2 10.0 1.064 100.0 1.927 130.0 1.503
Layer 3 20.0 9.943
noise10_t-1/2b
Layer 1 30.0 1.016 30.0 1.039 30.0 1.039
Layer 2 10.0 1.046 100.0 1.497 130.0 1.306
Layer 3 20.0 3.972
noise10_t-1/2c
Layer 1 30.0 1.015 30.0 1.037 30.0 1.037
Layer 2 10.0 1.033 100.0 1.242 130.0 1.163
Layer 3 20.0 1.391
Conductive Layer
Depth [m]
Resistivity [Ohm-m]
Close
Help

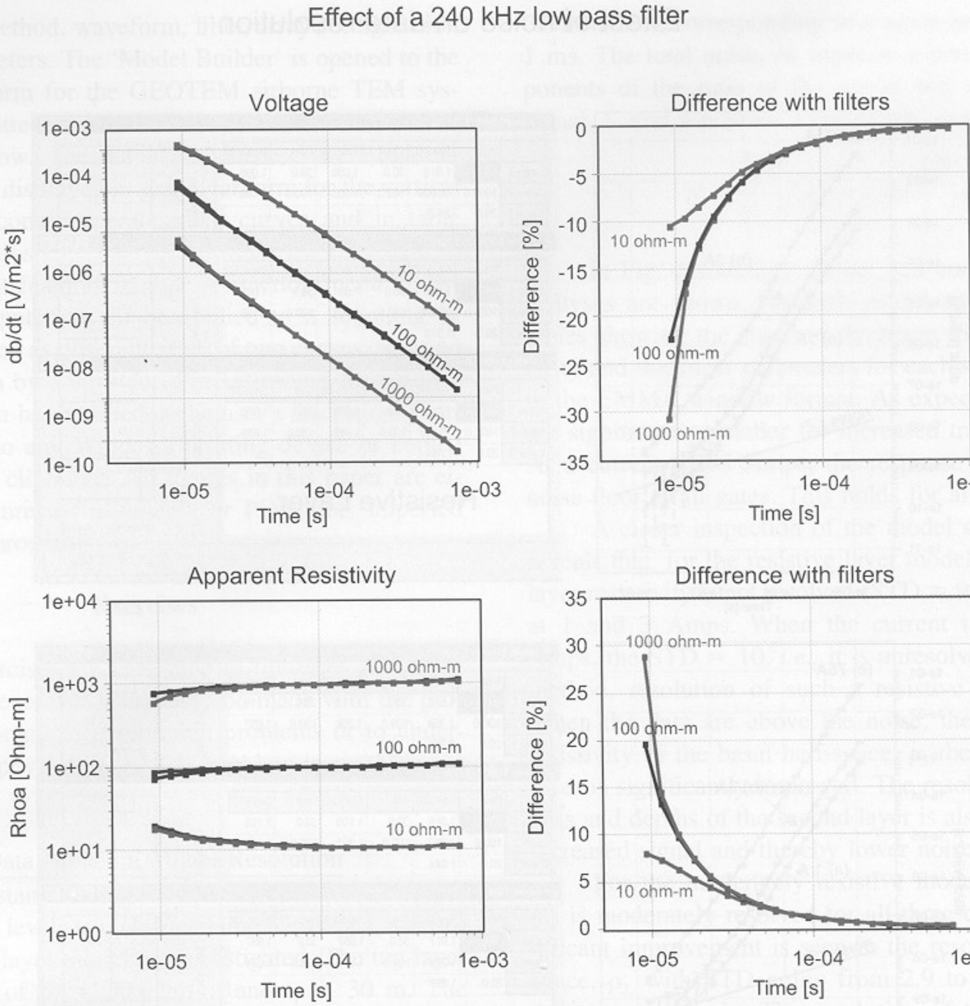

Figure 3. The effect of a 240 kHz LP filter on the early-time TEM response. Voltage and apparent resistivity soundings for 10, 100 and 1000 ohm-m half spaces are shown together with the corresponding difference percentage with the filter.

strength increases parameter resolution, but this modeling exercise shows specifically what one can hope to achieve by increasing the transmitter current. For a resistive layer and the basal half-space for all models, there is a significant increase in resolution of layer resistivity. The resolution of the thickness of a conductive layer was also notably enhanced.

Effect of Low-Pass Filters on TEM Measurements

Low-pass (LP) filters are used in TEM systems to improve the signal-to-noise ratio and, hence, the depth of exploration. Effersø *et al.* (1999) and Auken *et al.* (2000) have shown that filters must be included in an inversion scheme to avoid model distortions. With forward modeling, we can estimate the percentage of distortion to be expected at early times and calculate the model parameter resolution for a given LP-filter.

A 240 kHz LP filter, typical for a PROTEM 47 system, is used to calculate the response of a 10, 100 and 1000 ohm-m half space for a 30 by 30 m central-loop configuration on the surface of the earth. The voltage and apparent resistivity sounding curves, with and without the filter, along with plots of the percentage difference, are shown in Fig. 3. Although not easily visible in the sounding curves, a difference of nearly 30% is possible for a resistive earth. Even for a conductive half-space, a difference of more than 10% is seen in the response with the filter present. For all values of resistivity, the distortion persists to about 30 μsec.

LP filters with varying cut-off frequency will have different effects on different earth structures and will affect the ability of the system to resolve a given parameter. In Fig. 4, four filters—240, 100, 30 and 10 kHz—are used for a three-layer model. The 40 m thick, 1000 ohm-m top layer is followed by a 100 ohm-m, 60 m thick layer underlain by a 10 ohm-m half-space. As the cut-off frequency decreases, the effect of the filters becomes progressively more

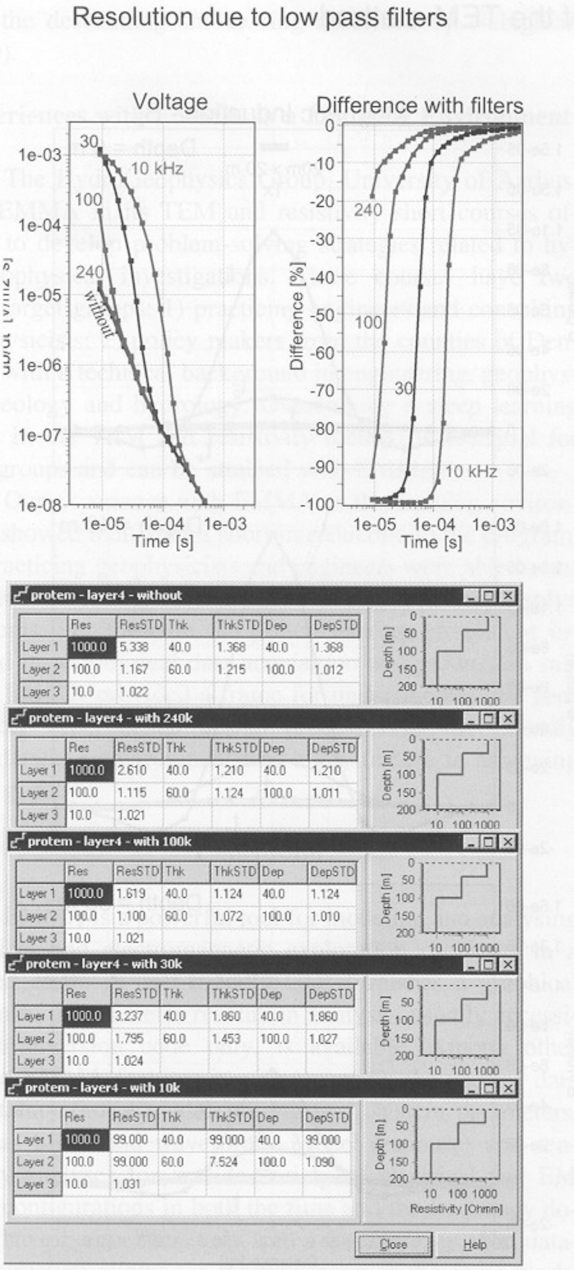

Figure 4. The effect of filtering on parameter resolution. Voltage response for 4 LP filters and corresponding percent difference and analysis tables for a three-layer earth.

pronounced, as is apparent in the voltage sounding curves and percentage difference plots. What is not so obvious is that the 100 kHz filter is optimal to resolve the section. Inspection of the analysis table shows that, with no filter and with the 240 and 30 kHz filter, the top layer is poorly resolved. The layer is also not resolvable with the 10 kHz filter. However, with the 100 kHz filter, the resolution of ρ_1 is moderate with STD = 1.7, and t_1 is well resolved with STD = 1.1. Parameter resolution is severely undermined by the use of the 10 kHz filter for all but the resistivity of the basal half space.

The explanation of the enhanced resolution of the near-surface parts of the model is that information is delayed in the LP filter until the Earth's response is sampled. The receiver coil and all the amplifiers are open at all times; the LP filter is charged with both the primary signal from the turn-off ramp and the Earth's response occurring from the start of the ramp to the first time gate. Thus, the LP filter delays information from very early times to later times where it is measured.

Physics of the TEM Method—Diffusion Currents in the Earth

In addition to its purpose of solving exploration problems, EMMA can be used as a teaching tool. Understanding the electric and magnetic fields that provide the measured quantities gives insight into the quality and nature of the data. Figure 5 shows profiles of the horizontal component of the electric field, E_y, and the vertical magnetic induction, B_z, due to a 20 by 20 m loop on the surface of a 100 ohm-m half space. Profiles are computed across the center of the loop, so that the only non-zero components are B_z and E_y. The profiles are calculated at depths of $z = 0$, 40 and 80 m, and at times of $t_1 = 14.5$, $t_2 = 29.0$, $t_3 = 58.0$ and $t_4 = 111.5$ μsec after the current is shut off. Beneath the B field profiles is a plot of the time derivative, *db/dt,* which is the commonly measured TEM response. The *db/dt* profile is calculated on the surface of the earth at the same gate center times as are the B_z and E_y profiles. Beneath the E field, plots are shown of the *db/dt* voltage sounding curves for 3 depths of $z = 0$, 40 and 80 m at $x = 0$ m measured below the center of the transmitter loop.

According to Maxwell's equations and the constitutive relationships (Ward and Hohmann, 1988), the E and B fields are related through Farday's Law. The electrical current is proportional to the E field and the conductivity of the host. The current moving counterclockwise shows a positive and a negative maximum on each side of the loop in the E field plots. The magnitudes of the fields decay rapidly with time. On the surface, the E field has just the positive and negative peaks, going to zero with no oscillations. At depth, lobes appear on each side of the main peaks, so that the lobes are almost equal in magnitude to the main peaks at a depth of 80 m. The corresponding B field shows a single positive peak at the center of the loop with side lobes. It is interesting to observe that the field strength is greater at a depth of 40 m than it is on the surface, but has been significantly reduced at a depth of 80 m for the earliest time.

The commonly measured quantity of *db/dt* is shown as profiles on the surface and as soundings at three depths. Note here that the zero crossings move out with time as

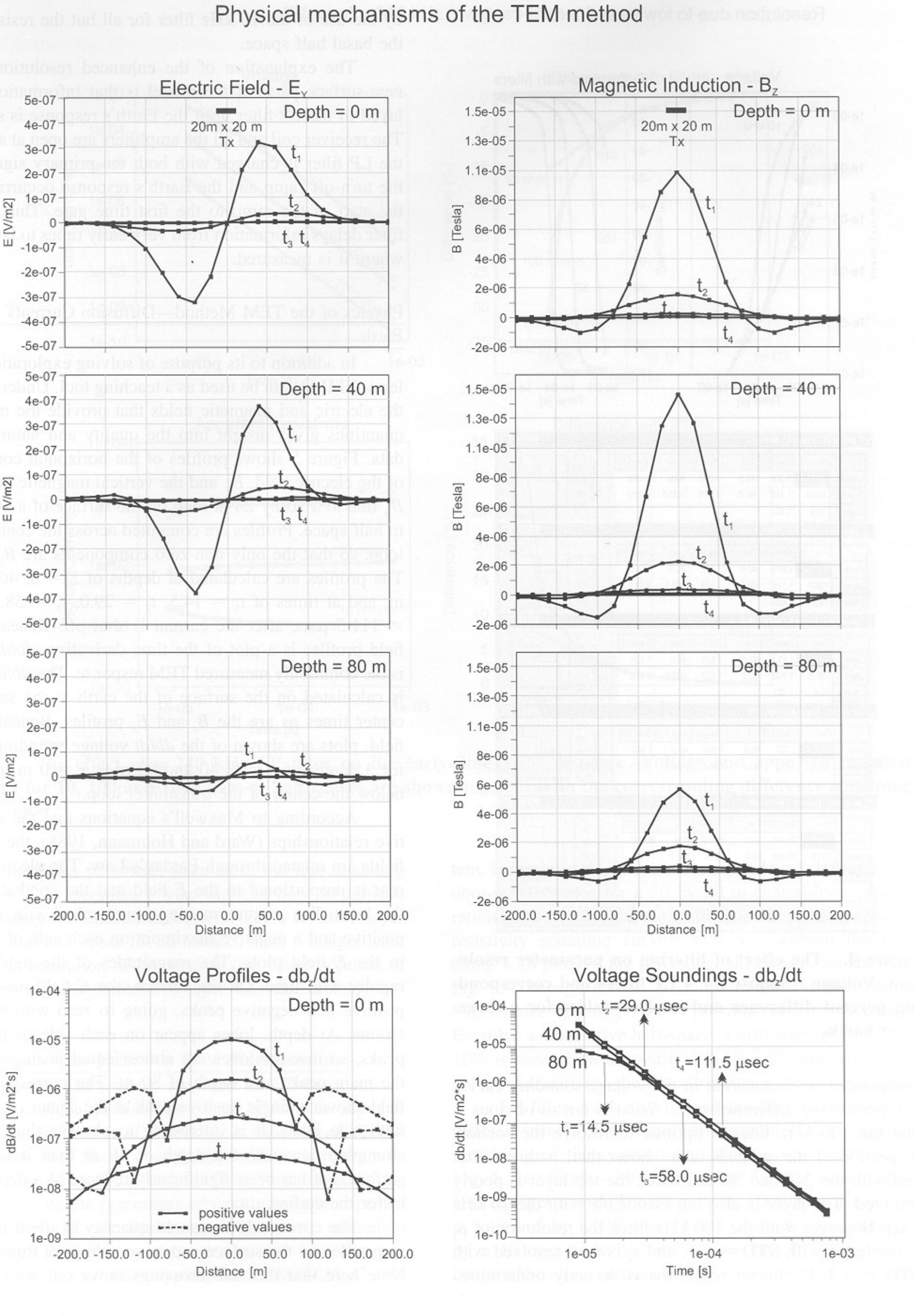
Physical mechanisms of the TEM method
Electric Field - E_y
Magnetic Induction - B_z
Depth = 0 m
Depth = 40 m
Depth = 80 m
20m x 20 m
Tx
t_1
t_2
t_3
t_4
E [V/m2]
B [Tesla]
Distance [m]
Voltage Profiles - db_z/dt
Voltage Soundings - db_z/dt
dB/dt [V/m2*s]
db/dt [V/m2*s]
positive values
negative values
0 m
40 m
80 m
t_1=14.5 μsec
t_2=29.0 μsec
t_3=58.0 μsec
t_4=111.5 μsec
Time [s]

does the descending smoke ring described by Nabighian (1979).

Experiences with EMMA as a Learning Environment

The HydroGeophysics Group, University of Aarhus, uses EMMA in its TEM and resistivity short courses offered to develop problem-solving strategies related to hydrogeophysical investigations. These courses have two main target groups: 1) practicing engineers and consulting geophysicists; 2) policy makers from the counties of Denmark with a technical background in engineering, geophysics, geology and hydrology. Overcoming a steep learning curve in the TEM and resistivity method is essential for both groups and can be attained with EMMA.

Our experience with EMMA as the learning environment showed that, after a short introduction to the program, the practicing geophysicists and engineers were able to understand the principle behind the TEM method and to solve problems. For those in the policy making group, not involved in geophysical data acquisition and production surveys, EMMA provided a frame for understanding the geophysical experimental design process. The user-friendly GUI database environment was a key feature in achieving these goals.

Conclusion

EMMA is a powerful tool for modeling and analysing electrical and electromagnetic exploration problems in a layered earth. A user-friendly GUI furnishes a graphical response. A parameter resolution analysis, usually accessible in inversion code only, is available. Among other unique EMMA features is assignment by the user of data uncertainty (noise models) along with system parameters, such as filters and waveforms. Model responses and sensitivity analyses for a wide variety of electrical and EM array configurations in both the time and the frequency domain have been extensively tested for accuracy. The database structure allows for multiple users in the same workspace making it ideal for educational purposes.

To illustrate the versatility, the TEM method was analyzed in 3 exercises: 1) mapping of noise to model parameters, 2) analyzing the effect of LP filters in data resolution and 3) an examination of the physics of the electric, magnetic intensity and time derivative of the magnetic intensity field. An experimentally determined noise model, valid for a Geonics PROTEM 47, reveals poor resolution of a certain earth structure. Low-pass filters contain early-time information enhancing the resolution of shallow structures. Understanding the relationship of the electric and the magnetic field increases the understanding of the measured response, and hence the interpretation of data.

EMMA is freely available on-line at http://www.hgg.au.dk for use by geologists, engineers and hydrologists as well as practicing geophysicists, and by the academic community for educational purposes. The program installation files include both the exercises and the EMMA workspace used in the TEM short courses.

Acknowledgments

We wish to thank the counties of Denmark for their financial support of the development of EMMA, Prof. Bo Holm Jacobsen for his help in formulating the solution analysis as well as his constructive comments in reviewing the manuscript. We also wish to thank Dr. Michael Hoversten and Prof. Frank Morrison for their encouragement for the formulating of the general frequency domain solutions. This work was done in 1995 by one of the authors, E. Auken. BA Lone Davidsen has patiently corrected and enhanced the language in the manuscript. Finally we are grateful for the constructive feedback we received from the participants in the TEM and resistivity short courses in hydrogeophysics held in 2000 and 2001.

References

Anderson, W.L., 1975, Improved digital filters for evaluating Fourier and Hankel transform integrals: US Geological Survey Report USGS-GD-75-012, 26P.

Asten, M.W., 1987, Full transmitter waveform transient electromagnetic modeling and inversion for soundings over coal measures: Geophysics **52**, 279–288.

Auken, E., Sørensen, K., Thomsen, P., and Effersø, F., 2000, Optimized model resolution using low pass filters in TDEM soundings: Proceedings of the Symposium on the Application of Geophysics to Engineering and Environmental Problems, 477–484.

Bankey V., and Anderson, W.L., 1995, A bibliography of some geophysical computer programs, databases, and maps from the U.S. Geological Survey, 1971–1994: USGS Open-File Report 95-77.

Boyd, T.M., and Romig, P.R., 1997, Cross-disciplinary education: The use of interactive case studies to teach geophysical exploration: Computers and Geosciences, **23** (5), 593–599.

Christensen, N.B., 1990, Optimized fast Hankel transform filters: Geophysical Prospecting **38**, 545–568.

←

Figure 5. Understanding of the physical mechanisms of the TEM method: Electric field (left) and magnetic induction (right) profiles centered on a 20 m by 20 m loop source over a 100 ohm-m half space. Profiles are for depths of 0, 40 and 80 m; times are at 14.5, 29.0, 58.0 and 111.5 μsec. Profile (left) and soundings (right) are also shown for the time derivative of the induction, db/dt.

Christensen, N.B., and Auken, E., 1992, Simultaneous electromagnetic layered model analysis: in Jacobsen, B.H., Ed., Proceedings of the Interdisciplinary Workshop 1. University of Aarhus, Denmark, GeoSkrifter **41**, 49–56.

Effersø, F., Auken, E., and Sørensen, K.I., 1999, Inversion of band-limited TEM responses: Geophysical Prospecting, **47**, 551–564.

Fitterman, D.V., and Anderson, W.L., 1987, Effect of transmitter turn-off time on transient soundings: Geoexploration **24**, 131–146.

Geonics Limited, 2001, http://www.geonics.com/tdem.html#TEM47

Jackson, D.D., 1979, The use of a priori data to resolve non-uniqueness in linear inversion: Geophys. J.R. Astr. Soc., **57**, 137–157.

Johansen, H.K., 1977, A man computer interpretation system for resistivity soundings over a horizontally stratified earth: Geophysical Prospecting, **25**, 667–691

Johansen, H.K., and Sørensen, K., 1979, Fast Hankel transforms: Geophysical Prospecting **27**, 876–901.

Jupp, D.L.B., and Vozoff, K., 1977, Resolving anisotropy in layered media by joint inversion: Geophys. Prosp., **25**, no. 03, 460–470.

Knight, J.H., and Raiche, A.P., 1982, Transient electromagnetic calculations using the Gaver-Stehfest inverse Laplace transform method: Geophysics, **47**, 47–50.

Menke, W., 1989, Geophysical Data Analysis: Discrete Inverse Theory. International Geophysics Series, Volume 45, Academic Press, San Diego, CA.

Munkholm, M.S., and Auken, E., 1996, Electromagnetic noise contamination on transient electromagnetic soundings in culturally disturbed environments: Journal of Environmental & Engineering Geophysics, **1** (2), 119–127.

Nabighian, M.N., 1979, Quasi-static transient response of a conducting half-space—An approximate representation: Geophysics, **44** (10), 1700–1705.

Newman, G.A., Hohmann, G.W., and Anderson, W.L., 1986, Transient electromagnetic response of a three-dimensional body in a layered earth: Geophysics **51**, 1608–1627.

Oldenburg, D.W., 2001, University of British Columbia-Geophysical Inversion Facility Inversion and Modelling of Applied Geophysical Electromagnetic data (IMAGE) Consortium: http://www.geop.ubc.ca/ubcgif/research/image/index.html

Pinto, V., Rivero, L., and Casas, A., 2000, Teaching oriented geophysical software: Computers and Geosciences, **26** (7), 809–814.

Raiche, A.P., 1984, The effect of ramp function turn-off on the TEM response of layered earth: Exploration Geophysics, **15**, 37–41.

Raiche, A.P., 2001, CSIRO EM Modelling Program: http://www.csiro.au/

Telford, W.M., Geldart, L.P., and Sheriff, R.E., 1995, Applied Geophysics. Cambridge University Press, New York.

Tarantola, A., and Valette, B., 1982, Generalized nonlinear inverse problems solved using a least squares criterion: Reviews of Geophysics and Space Physics, **20**, 219–232.

Ward, S.H., and Hohmann, G.W., 1988, Electromagnetic theory for geophysical applications: in Nabighian, M.N., Ed., Electromagnetic Methods in Applied Geophysics, 01: Society of Exploration Geophysicists, 131–312.

Zhdanov, M.S., 2001, University of Utah Consortium for Electromagnetic Modeling and Inversion: http://www.mines.utah.edu/~wmcemi/

Appendix A

An overview of the source-receiver configurations available in EMMA is shown in Table A1.

Technically, the EMMA program is an interface to the FORTRAN 95 program inversion and analysis program em1dinv. Em1dinv is divided into two main modules; an inversion and model parameter analysis module and a forward response module. The forward response module is subdivided into a resistivity module, a MT module, and a frequency domain module. The time domain responses are calculated by a Fourier transform (using digital filters, Johansen and Sørensen (1979)) of the frequency domain responses; hence the time domain responses are evaluated by repeated calls to the frequency domain module. The frequency domain module is subdivided into kernel functions specified for a given source-receiver combination. All kernel functions apply common layer recursion subroutines for calculating the layer impedances (Ward and Hohmann, 1988).

The frequency domain sources were implemented by one of the authors (Esben Auken) in 1995 at the Engineering Geosciences group, University of Berkeley, California,. The original code was called em1dsh—a sheets code available from the Lawrence Berkeley Lab. by Dr. Michael Hoversten.

At that time great effort was put into verifying the new numerical implementations against other codes. The dipole sources were tested against a code called em1d by Prof. K. H. Lee, Lawrence Berkeley Lab. In general, by comparison to analytic half space responses, the responses calculated by em1dsh were more accurate at high frequencies compared to em1d. This is due to the enhanced digital filters calculated by Christensen, 1990, compared to the filters by Andersen (1975) used in the em1d code.

The finite loop sources and the grounded electric dipoles were compared to the 1D part of the 3D integral equation code by Newman *et al.* (1986). This code was also used to verify the infinite electric line sources. In general, the responses were slightly more accurate at high frequencies when compared to analytic half space responses.

The accuracy of any numerical implementation of electromagnetic responses is dependent on the resistivity model and the density of the digital filters used to carry out the numerical integration of the kernel function.

The absolute numerical accuracy can be evaluated only by comparing the responses to analytic solutions. The numerical accuracy in em1dinv is adjusted to about 0.1%

Table A1. The table shows available source-receiver configurations in EMMA. The configurations in bold are already implemented in the underlying FORTRAN 95 code, em1dinv, but they have not been transferred to the EMMA menu system. The HGG group plans to do that in the fall of 2002.

Source group	Source configuration	Receiver	Source location	Receiver postition	Domain
Dipole	Vertical magnetic dipole	Dipole: E^x, E^y, H^x, H^y, H^z (or B)	Everywhere	Everywhere	Frequency and time
	Vertical electric dipole	Dipole: E^x, E^y, E^z, H^x, H^y (or B)	Everywhere	Everywhere	Frequency and time
	Horizontal electric dipole	Dipole: E^x, E^y, E^z, H^x, H^y, H^z (or B)	Ground surface or in the air	Everywhere	Frequency and time
Loop	Retangular loop	Dipole: E^x, E^y, H^x, H^y, H^z (or B)	Ground surface or in the air	Everywhere	Frequency and time
	Cicular center	Dipole: E^x, E^y, H^x, H^y, H^z (or B)	Ground surface or in the air	Everywhere	Frequency and time
	Circular offset	Dipole: E^x, E^y, H^x, H^y, H^z (or B)	Ground surface or in the air	Everywhere	Frequency and time
Wire	Finite length grounded x-directed dipole	Dipole: E^x, E^z, H^y, H^z (or B)	Ground surface	Everywhere	Frequency and time
	Finite length grounded y-directed dipole	Dipole: E^y, E^z, H^x, H^z (or B)	Ground surface	Everywhere	Frequency and time
	Infinite x-directed line source	**Dipole: E_x, H_y, H_z (or B)**	**Ground surface**	**Everywhere**	Frequency and time
	Infinite x-directed line source	**Dipole: E_y, H_x, H_z (or B)**	**Ground surface**	**Everywhere**	Frequency and time
Resistivity	Schlumberger	Apparent resistivity or potentials	Ground surface	Ground surface	
	Wenner	**Apparent resistivity or potentials**	**Ground surface**	**Ground surface**	
	Pole-pole	**Apparent resistivity or potentials**	**Ground surface**	**Ground surface**	
	Dipole-dipole	**Apparent resistivity or potentials**	**Ground surface**	**Ground surface**	
Magnetolluric		**Apparent resistivity or dipole E_x, E_y, H_x, H_y**		**Ground surface or in the ground**	

in the frequency domain and 0.5–1.0% in the time domain. In general, the frequency domain solutions break down at frequencies above approx. 1 GHz. The time domain solutions break down at times earlier than approx. 4.0μs.

The numerical accuracy can be enhanced by using more densely sampled digital filters, which, however, increases the response evaluation time proportional to the sampling density. This only applies to the digital filters by Johansen and Sørensen (1979). These filters increase the numerical accuracy proportional to $\exp(-\Delta)$, where Δ is the logarithmic sampling distance.

The implementation of waveforms and filters for the time domain responses are verified against the SELMA code (Christensen and Auken, 1992). This code is limited to time domain solutions for the circular central and circular offset loop configurations. Nevertheless, this check should be sufficient because of the modular structure of em1dinv. When waveforms and filters are applied to the responses, the same module is used independent of the source-receiver type.

No numerical code can be guaranteed bug-free. The HGG group is certainly aware of that, and we will therefore enhance the em1dinv code if and when users report erroneous responses.